Article

Not peer-reviewed version

Common Chemical Plasticizer di(2-Ethhylhexyl) Phthalate Exposure Exacerbates Coxsackievirus B3 Infection

Ramina Kordbacheh , Madelyn Ashley , William D Cutts , Taryn E Keyzer , Shruti Chatterjee , Tyler J Altman , Natalie G Alexander , Tim E. Sparer , Brandon J. Kim , Jon Sin *

Posted Date: 19 September 2024

doi: 10.20944/preprints202409.1523.v1

Keywords: coxsackievirus B3; di(2-ethylhexyl) phthalate; proviral; environmental factors

 doi:10.20944/preprints202409.1523.v1

Article

Common Chemical Plasticizer di(2-ethhylhexyl) Phthalate Exposure Exacerbates Coxsackievirus B3 Infection

Ramina Kordbacheh [1], Madelyn Ashley [1], William D. Cutts [1], Taryn E. Keyzer [1], Shruti Chatterjee [1], Tyler J. Altman [1], Natalie G. Alexander [1], Timothy E. Sparer [2], Brandon J. Kim [1] and Jon Sin [1,*]

[1] Department of Biological Sciences, University of Alabama, Tuscaloosa, AL, USA
[2] Department of Microbiology, University of Tennessee, Knoxville, TN, USA
* Correspondence: jjsin@ua.edu

Abstract: Di(2-ethhylhexyl) phthalate (DEHP) is a common plastic rubberizer. DEHP leaches from plastic matrices and is under increasing scrutiny as numerous studies have linked it to negative human health manifestations. Coxsackievirus B3 (CVB) is a human pathogen that typically causes subclinical infections but can sometimes cause severe diseases such as pancreatitis, myocarditis, and meningoencephalitis. Though CVB infections are common, severe illness is relatively rare, and it is unclear what factors mediate severity of disease. Here we show that DEHP drastically increases CVB infection in a variety of human cell types. While not entirely clear what cellular processes underly DEHP's proviral properties, we observe that DEHP may subvert CVB-induced interferon signaling and elevate levels of interferon-induced transmembrane proteins which appear to bolster CVB infection. We hypothesize that DEHP may represent a major environmental factor associated with the severity of CVB infection. Further understanding how DEHP exacerbates infection may better elucidate its potential role as a proviral environmental factor.

Keywords: Coxsackievirus B3 (CVB); Di(2-ethhylhexyl) phthalate (DEHP); proviral; environmental factors.

Introduction

Di(2-ethylhexyl) phthalate (DEHP) is one of the most common plasticizers applied to polyvinyl chloride (PVC) to rubberize this typically hard plastic and make it more pliable [1,2]. DEHP is regularly used in a number of household items as well as food packaging and medical products like blood bags, tubing, disposable gloves, and oxygen masks [3–7]. As DEHP is not strongly bound to PVC matrices, it can readily leach out of plastics and can increase the longevity of stored blood [8,9]. This is one of the primary reasons that DEHP is still a standard component of blood bags, despite ongoing efforts to identify alternative plasticizers. Because DEHP accumulates both in the environment and within bodily tissues, and there are links to human health abnormalities such as liver cancer, cardiovascular diseases, and the reproductive system, there is a push to transition away from its usage [8,10,11]. Studies on the association between DEHP and infectious disease are currently very limited. However, patients exposed to increased concentrations of DEHP have exacerbated dengue virus infections and associated clinical symptoms [12].

To investigate this possible connection between DEHP and viral infections our initial step was to use coxsackievirus B3 (CVB) as a model RNA virus. CVB is a positive sense single-stranded RNA virus and a member of the *Enterovirus* genus and *Picornavaridae* family. Like other picornaviruses, CVB is a naked virus lacking a lipid envelope [13]. Human exposure to CVB is relatively common worldwide and is typically either asymptomatic or leads to mild subclinical illness including rash, fever, or upper-respiratory illness. Occasionally though, CVB infections can be much more severe

 doi:10.20944/preprints202409.1523.v1

resulting in potentially fatal systemic diseases such as myocarditis, pancreatitis, and meningoencephalitis [14,15]. All ages are susceptible to CVB infection and disease, however the most affected group is typically children under 2 years of age [16]. Though it is thought that a large proportion of the population has at some point been infected with CVB, cases of severe disease are comparatively low. Generally, CVB disease manifestation may be influenced by various genetic and environmental factors [17,18]. Despite this, there is little known what these risk factors are.

In this study, we examined the effect of DEHP exposure on CVB infection in three different human cell types: cervical cancer cells (HeLa), induced pluripotent stem cell-derived brain-like endothelial cells (iBEC), and colon carcinoma cells (Caco-2). We additionally tested the effects on mouse atrial cardiomyocytes (HL-1). We found that media concentrations of 40 μg/mL DEHP had no observable impact on cell growth and viability in any of the cell types. However, this dose of DEHP substantially enhanced CVB infection compared to vehicle-treated controls. In several of these cell types, increased infection appears to be a byproduct of dramatically enhanced viral spread, as infected cell number and extracellular viral titers were disproportionately higher than intracellular viral protein content. Because CVB is a leading cause of meningoencephalitis, we further interrogated cellular factors in iBECs to determine the contributions to DEHP-mediated increases in infection. We found that DEHP significantly blunted interferon regulatory factor 7 (IRF7) in response to viral infection. We further examined interferon-related responses and assessed levels of interferon-induced transmembrane proteins (IFITMs) in HeLas and iBECs exposed to DEHP. Interestingly, we found that IFITM2/3 was increased with DEHP treatment, and genetically silencing *IFITM2* and *IFITM3* significantly reduced infection. Little is currently known regarding the relationships between CVB and IFITMs, however our data suggest that IFITM2/3 may support infection. To determine if DEHP's proviral effects are specific to CVB or viruses in general, we repeated these experiments with murine CMV (MCMV), a large DNA virus, and the bacterium, group B streptococcus (GBS). In all, we show that CVB and GBS infection is significantly enhanced following DEHP exposure while MCMV is not. Further studies are needed to fully understand the underlying mechanisms that contribute to the pro-viral/bacterial nature of DEHP and to elucidate the physiological impact of DEHP on disease.

Materials and Methods

Cell culture. HeLa human cervical cancer cells were cultured in Dulbecco's Modified Eagle's Medium (DMEM) (Sigma-Aldrich, D6429) complete medium containing 10% fetal bovine serum (FBS) (Avantor, 89510-166) and 100 μg/mL penicillin/streptomycin (Sigma-Aldrich, A5955). Human induced pluripotent stem cell (iPSC)-derived brain-like endothelial cells (iBECs) were cultured in human endothelial cell serum-free medium containing 1% B27 (Gibco, 17504044). Colorectal cancer cells (Caco-2s) were cultured in DMEM containing 10% FBS. Mouse atrial cardiomyocyte cells (HL-1s) were cultured in Claycomb Medium (Sigma-Aldrich, 51800C) containing 10% FBS, 100 μg/mL penicillin/streptomycin, 0.1 mM norepinephrine (Thermo Scientific, L08087.03), and 2 mM L-glutamine (Gibco, 25030-081). 10.1 Mouse embryonic fibroblasts (Dr. Ianzini, University of Iowa) [19] were cultured in DMEM containing 10% FBS and 100 μg/mL penicillin/streptomycin. All the cell types were cultured at 37°C in 5% CO2.

Differentiation of induced Pluripotent Stem Cells into Brain-like Endothelial Cells. iPSCs (WiCell Research Institute, WI, USA, ID: WISCi004-B) were cultured on Matrigel-coated plasticware, maintained in StemFlex medium (Gibco, A3349401), and routinely passaged. Once iPSCs reached 80% confluency, cells were differentiated according to previously published protocols [20–22]. Cells were maintained in a StemFlex medium for 3 days. To initiate differentiation into brain-like endothelial cells, cells were then cultured in un-conditioned medium for 6 days. Lastly, cell media was changed to endothelial cell medium supplemented with 10 μM retinoic acid (Sigma-Aldrich, R2625) to enhance blood-brain barrier phenotypes such as high TEER [22]. Purified iBECs were maintained in an endothelial cell medium containing 1% B27 (Gibco, 17504044) on extracellular matrix-coated plasticware.

 doi:10.20944/preprints202409.1523.v1

Generation of enhanced green fluorescent protein-expressing coxsackievirus B3 viral stocks. Viral stocks were established using the previously described enhanced green fluorescent protein (EGFP)-containing pMKS1 plasmid (Ralph Feuer, San Diego State University, CA, USA) [23]. This plasmid not only contains the entire backbone of the myocarditis Nancy H3 variant of CVB3, but also has a unique SfiI restriction site upstream of the viral backbone wherein EGFP was inserted. Viral transcripts were generated by linearizing the plasmid by digesting with ClaI restriction enzyme and performing in vitro transcription on digested products via the mMessage mMachine T7 Transcription Kit (Thermo Fisher Scientific) following manufacturer's protocol. Transcription products were then transfected into HeLa cells using Lipofectamine 2000 (Thermo Fisher) following manufacturer's protocol. Once 50% of cells displayed viral EGFP, cells were scraped, media and cells collected and subjected to three freeze-thaw cycles, and cellular debris was removed by centrifuging at 800 x *g*. Supernatants were referred to as "passage 1". Viral stocks were expanding by overlaying "passage 1" virus onto fresh HeLa cells which were similarly harvested, freeze-thawed, and clarified once 50% of cells displayed viral EGFP. The resulting supernatant was deemed "passage 2" and used for downstream infection experiments. HeLa cell growth medium was used for mock infections.

DEHP treatment. Di(2-ethylhexyl) phthalate (DEHP) (Sigma-Aldrich, 80030-5ML) was diluted in dimethyl sulfoxide (DMSO) (Sigma-Aldrich, D8418) at a concentration of 40 mg/mL. HeLas, iBECs, Caco-2s, HL-1s, and 10.1 MEFs were treated with 40 μg/ml DEHP by diluting DEHP stock 1:1000 in respective cell medium for 24 hours prior to infecting with EGFP-CVB at indicated multiplicities of infection for indicated amounts of time. Vehicle controls were treated with equivalent volume DMSO. 40 μg/mL DEHP concentration is considered within a clinically relevant range and was also chosen for cell treatment based on a dose curve including 10, 20, 30, 40, and 80 μg/mL performed on HeLa cells [24,25]. Though no cell death was observed at any concentration tested, 80 μg/mL resulted in reduced cell number after treatment.

Western blot. Cells were harvested in radioimmunoprecipitation assay (RIPA) buffer (50 mM Tris-HCl (Sigma-Aldrich, 10812846001), 1% NP-40 (Sigma-Aldrich, 74385), 0.5% deoxycholate, 0.1% sodium dodecyl sulfate, 150 mM sodium chloride (Sigma-Aldrich, 13423), 2 mM ethylenediaminetetraacetic acid) and protease inhibitor cocktail (Thermo Scientific, A32965). Protein concentrations were determined using bicinchoninic acid assay (Thermo Scientific, 23228). Equal amounts of protein were prepared in Laemmli sample buffer (1% bromophenol blue (Allied Chemical, 0332), 1.5 M Tris-Cl pH 6.8, glycerol (Sigma-Aldrich, G5516), β-mercaptoethanol (Fisher Scientific, BP176-100) and then separated in 4–12% Bis-Tris protein gels. Proteins were then transferred to nitrocellulose membranes, and membranes were stained with Ponceau S solution (Sigma-Aldrich, SLCQ5486) and imaged via iBright FL1500 Imaging System (Invitrogen, Waltham, MA, USA). Membranes were blocked in blocking solution (Tris-buffered saline containing 0.1% Tween-20 (Sigma-Aldrich, P1379) (TBS-T) and 3% Bovine serum albumin (BSA) (Sigma-Aldrich, A9647), and placed in primary antibody diluted in blocking solution and incubated overnight at 4°C. Primary antibodies used in this study were as follows: VP1 (Mediagnost, Cox mAB 31A2, 1:2000), IRF7 (Santa Cruz, sc-74472, 1:1000), IRF3 (Santa Cruz, sc-33641, 1:1000) and IFITM2/3 (Cell Signaling, E5F8C, 1:1000). Membranes were then washed in TBS-T and incubated in anti-mouse secondary antibody (Sigma-Aldrich, 12-349, 1:3000) and anti-rabbit secondary antibody (Sigma-Aldrich, F9887, 1:3000). Membranes were again washed in TBS-T, and after applying SuperSignal West Dura Extended Duration chemiluminescent substrate, were imaged via iBright FL1500 Imaging System. Densitometry was performed using ImageJ software with background subtraction applied to all quantifications.

Plaque assay. Infectious tissue culture media was serially diluted in DMEM and 400 μL of each dilution was overlain onto confluent HeLa cell monolayers in 6 well plates. Following one hour incubation at 37°C with occasional rocking, cells were overlain with 4 mL 50:50 mixture of 1.2% molten agarose (VWR, 1855C495) and 2X DMEM and incubated at 37°C. After 48 hours, agar plugs were fixed for 20 minutes with 2 mL plaque fixative (25% acetic acid (Thermo Fisher Scientific, A38S-212) and 75% methanol (Sigma-Aldrich, 179337). Agar plugs were then removed, and cells were

 doi:10.20944/preprints202409.1523.v1

stained with 2.34% crystal violet solution (Sigma-Aldrich, C0775). Crystal violet was then washed off and viral plaques were counted.

MCMV plaque assays were carried out as previously described [26]. Briefly, MEF 10.1 cells were used to determine viral titers. Cells were plated in a six-well dish. Supernatants from treated or non-treated cells were serially diluted and added to MEF 10.1 cells and incubated for one hour. After incubation, the diluted virus was removed, and cells were overlaid with carboxymethyl cellulose (CMC) (Sigma-Aldrich, 419273) medium and incubated for 3-5 days. CMC was removed, and plates were stained with Coomassie blue (Sigma-Aldrich, G1041), and plaques were counted.

Cell viability. Supernatants from cultured cells were first collected in individual 15 mL conical tubes. Cells were then washed with phosphate-buffered saline (PBS) (Thermo Scientific, J60801.K7) and wash was added to respective conical tubes to ensure collection of already detached cells. Adherent cells were detached with Trypsin-EDTA (Thermo Fisher, 25200056) and collected in respective conical tubes. Cells were pelleted by centrifugation at 300 x *g* for 5 minutes. After resuspending cells in 1 mL fresh growth medium, equal volumes suspended cells and trypan blue solution (Invitrogen by Thermo Fisher Scientific, T10282) were combined, and viability was quantified using Countess 3 cell counter (Thermo Fisher Scientific, Waltham, MA, USA).

Flow cytometry. Supernatants from cultured cells were first collected in individual 15 mL conical tubes. Cells were then washed with PBS and wash was added to respective conical tubes to ensure collection of already detached cells. Adherent cells were detached with Trypsin-EDTA and collected in respective conical tubes. 10 mL growth medium was added to each conical tube and centrifuged at 500 x *g* for 10 minutes. Supernatant was discarded and cells were resuspended and fixed in 5 mL 4% paraformaldehyde (PFA) (Formaldehyde solution, 47608-1L-F). After 10 minutes fixation, cells were centrifuged at 500 x *g* for 10 minutes. Supernatant was discarded and cells were washed by resuspending in 10 mL PBS and centrifuging at 500 x *g* for 10 minutes. Supernatant was discarded and cells were resuspended in 500 µL fresh PBS. Cells were then filtered in filter tubes to ensure single cell suspension and analyzed via Attune NxT flow cytometer (Thermo Fisher Scientific, Waltham, MA, USA).

Transendothelial electrical resistance. Transendothelial electrical resistance (TEER) was carried out as previously described [20–22]. Briefly, iBECs were seeded on 6.5 mm transwell inserts in a 24 well plate. 24 hours before infection, cells were treated with DEHP or an equal concentration of DMSO. Transwells were then infected at MOI 1 with EGFP-CVB or mock infected. TEER was measured every 24 hours for 9 days using World Precision Instruments EVOM² Epithelial Voltohmmeter and World Precision Instruments Chopsticks Electrode Set STX2.

Bacterial adherence and infection assays. Adherence and invasion were quantified as described previously [27–29]. iBECs were seeded onto collagen-fibronectin-coated 24-well plates (Corning) and grown to a confluent monolayer. 24 hours prior to infection cells were treated with either DEHP or an equal concentration of DMSO. Overnight cultures of *S. agalactiae* were grown in Todd-Hewitt broth media. iBECs were then infected with *S. agalactiae* at an MOI of 10. During infection, cells were incubated at 37°C + 5% CO2. For adherence, cells were infected for 30 minutes, then washed 5x with sterile PBS to remove non-adherent bacteria. Following the washes, the wells were treated for 10 minutes with .25% trypsin-EDTA (VWR), and the mammalian cells were lysed with .025% Triton X-10 (Sigma-Aldrich, X100). The resultant suspensions were diluted and plated onto Todd-Hewitt agar (THA) plates. For invasion, cells were infected as above for 2 hours, followed by addition of 100 µg/mL gentamycin and incubated for an additional 2 hours at 37°C + 5% CO2. Cells are then washed 3x in sterile PBS and then lysed as above before being plated onto THA plates. Relative adherence and invasion were quantified with the following formula, (#CFU * dilution correction * volume correction) / (input CFU/well).

Small interfering RNA (siRNA) transfection. Scrambled siRNA (Santa Cruz Biotechnology, sc-37007), human *IFITM2* siRNA (Santa Cruz Biotechnology, sc-96760), and human *IFITM3* siRNA (Santa Cruz Biotechnology, sc-97053) were reconstituted in nuclease-free water following manufacturer-provided datasheet. siRNAs were transfected into HeLa cells using Effectene Transfection Reagent (Qiagen, 301425) according to manufacturer's guidelines for reagent volumes.

 doi:10.20944/preprints202409.1523.v1

After 48 hours of transfection, HeLa cell media was refreshed with DMEM complete medium. Cells were then infected with EGFP-CVB at MOI 0.001.

Quantification and statistical analysis. GraphPad Prism version 10.2.1 was used for all statistics calculations. For pair-wise comparisons, Student's t-tests were performed and for multiple comparisons, one-way ANOVA was performed. Statistical significance was accepted if $p<0.05$.

Results

Coxsackievirus B3 Infection Increases Following Di(2-ethhylhexyl) Phthalate (DEHP) Exposure

To begin interrogating the effects of Di(2-ethhylhexyl) phthalate (DEHP) exposure on Coxsackievirus B3 (CVB) infection, we treated three different human cell types with DEHP and infected them with enhanced green fluorescent protein expressing-CVB (EGFP-CVB). HeLa cells, iBECs, and Caco-2 cells were treated with 40 μg/mL DEHP for 24 hours and subsequently infected with EGFP-CVB. This concentration of DEHP is considered within a clinically relevant range [24,25], and it alone had no observable toxic effect on cell viability, proliferation, or morphology (Supplemental Figure S1). However, fluorescence microscopy on infected cells revealed substantially increased numbers of EGFP-positive cells in infected DEHP-treated groups compared to their corresponding infected DMSO-treated (vehicle) groups (Figure 1A). We also examined CVB infection following DEHP exposure on HL-1 cells and observed increased infected cell numbers 24 hours post-infection in the DEHP-treated group (Supplemental Figure S2A). To quantitatively validate these microscope-based observations, we performed flow cytometry on infected cells and indeed found that DEHP treatment significantly increased EGFP-positivity (Figure 1B). These results indicate that DEHP significantly enhances infected cell numbers following CVB exposure.

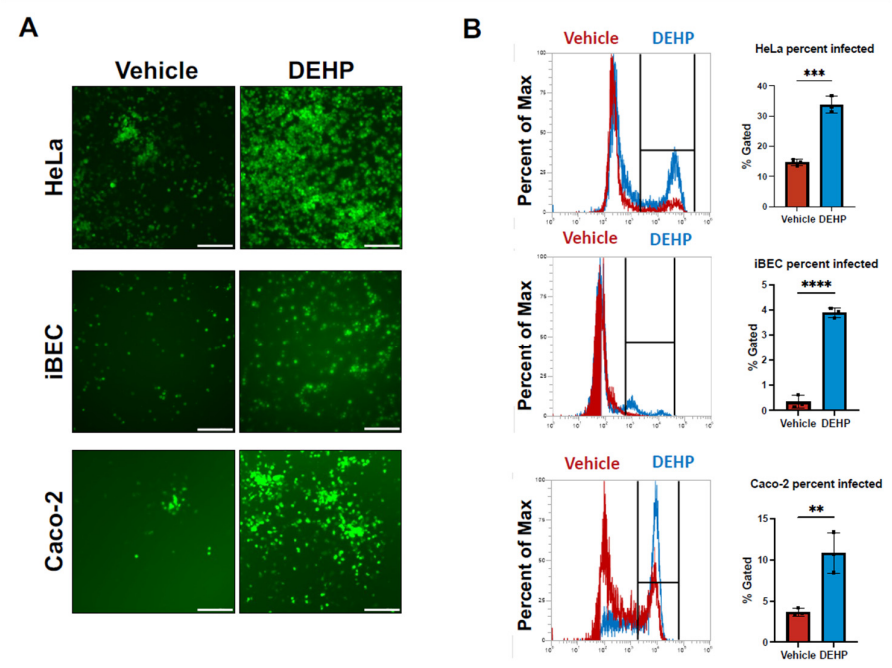

Figure 1. CVB infection increases following DEHP exposure. **(A)** Fluorescence microscopy detecting enhanced green fluorescent protein (EGFP) expression between HeLa cells (top), iBECs (middle), and Caco-2 cells (bottom) treated with 40 μg/mL DEHP or equivalent volume vehicle for 24 hours prior to infecting with EGFP-CVB at multiplicity of infection (MOI) of 0.001, 1, or 0.001 respectively for 24 hours or 48 hours (scale bars=100 μm). **(B)** Flow cytometry quantifying cells in **A.** Flow cytometry gates for quantification were defined using the termination of the fluorescent peak, at which the

 doi:10.20944/preprints202409.1523.v1

fluorescent signal was closest to zero, in a mock uninfected sample. This allowed for effective measurement of a shift in intensity or appearance of an infected population. (Student's t-test; n=3 per group; ** p<0.01, *** p<0.001, **** p<0.0001. Error bars represent standard deviation).

DEHP Enhances Viral Egress of CVB in Certain Cell Types

Next, we assessed whether DEHP altered intracellular and extracellular viral content following infection. Western blots on whole cell lysates revealed marked increases in viral capsid protein VP1 and substantially higher amounts of extracellular virus in HeLa cells (Figure 2A,B). In the case of iBECs, despite the previously observed increase in infected cells, intracellular VP1 content was not significantly altered in DEHP-treated cells (Figure 2C). Interestingly, extracellular viral titers were significantly elevated in iBECs exposed to DEHP (Figure 2D). HL-1s also showed disproportionately higher levels of extracellular viral titers following DEHP treatment (Supplemental Figure S2B,C). Caco-2 cells were the only cell type that did not exhibit an exaggerated elevation in CVB release, though both VP1 and viral titers in the media were still both significantly enhanced with DEHP (Figure 2E,F). Overall, the disparity in extracellular and intracellular viral load we observe in HeLas, iBECs, and HL-1s coupled with the dramatically increased infected cells (Figure 1) suggests that DEHP can greatly enhance viral spread.

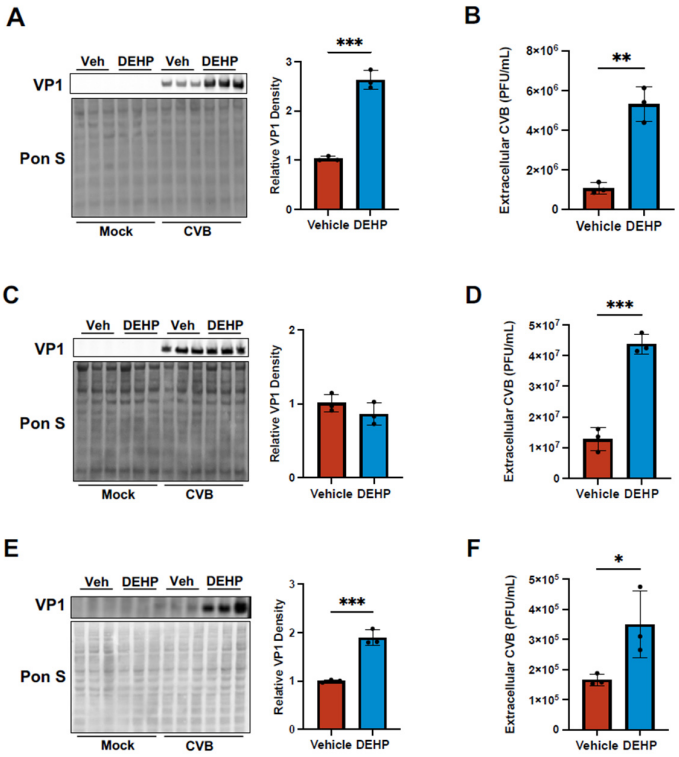

Figure 2. DEHP enhances viral egress of CVB. **(A)** Western blot detecting viral capsid protein VP1 in HeLa cells treated with DMSO (vehicle) or DEHP before infecting with EGFP-CVB or mock-infecting. Ponceau S (Pon S) stain is shown below. The densitometric quantification of VP1 is shown to the right. **(B)** Viral plaque assays enumerating infectious viral titers in tissue culture media from cells in **A**. **(C)** Western blot detecting VP1 in iBECs treated with vehicle or DEHP prior to infecting with EGFP-CVB or mock-infecting. Pon S stain is shown below. Densitometric quantification of VP1 is shown to the right. **(D)** Viral plaque assays enumerating infectious viral titers in tissue culture media from cells in **C**. **(E)** Western blot detecting VP1 in Caco-2 cells treated with vehicle or DEHP prior to infecting with EGFP-CVB or mock-infecting. Pon S stain is shown below. Densitometric quantification of VP1 is shown to the right. **(F)** Viral plaque assays enumerating infectious viral titers in tissue culture media

 doi:10.20944/preprints202409.1523.v1

from cells in **E**. (Student's t-test; n=3 per group; * p<0.05, ** p<0.01, *** p<0.001. Error bars represent standard deviation).

DEHP Suppresses CVB-Mediated Interferon Regulatory Factor 7 Induction in iBECs

According to a previous study assessing DEHP exposure in dengue virus-infected patients, higher urine DEHP concentrations correlated with exacerbated disease symptoms such as chills and gastrointestinal bleeding [12]. Furthermore, this study found that elevated DEHP concentrations correlated negatively with urine concentrations of IL-23 and plasma concentrations of IL-17, both of which are involved in host immunity towards dengue virus. Given that DEHP reportedly limits host antiviral responses, we sought to determine if suppression of antiviral immunity may contribute to enhanced CVB infection following DEHP treatment. Because CVB is a known neurotropic virus, we focused on infection in iBECs, a cell line with robust blood-brain barrier properties. We previously demonstrated a decline in barrier properties following CVB infection as indicated in this line as measured by a dramatic decrease in transendothelial electrical resistance (TEER)[30]. In CVB-infected iBECs we observed that DEHP caused a near complete loss of infection-induced loss of barrier integrity sooner than vehicle-treated cells (Figure 3A). At day 6 post-infection, we observed a significant decrease in infected groups, especially the CVB DEHP group (Figure 3B). In addition, the area under the curve quantification from day 0 to day 9 was significantly lower in the CVB DEHP group compared to the CVB Vehicle group (Figure 3C). We hypothesized that these differences could be due to DEHP alteration in cellular interferon responses. Western blotting revealed that interferon regulatory factor 7 (IRF7) was significantly elevated following CVB infection alone, however iBECs failed to induce IRF7 in the presence of DEHP (Figure 3D). Interestingly CVB infection or DEHP treatment of iBECs did not affect interferon regulatory factor 3 (IRF3), another central component of interferon-mediated antiviral signaling. These results suggest that suppression of antiviral immunity via IRF7 inhibition may contribute to DEHP-mediated proviral effects.

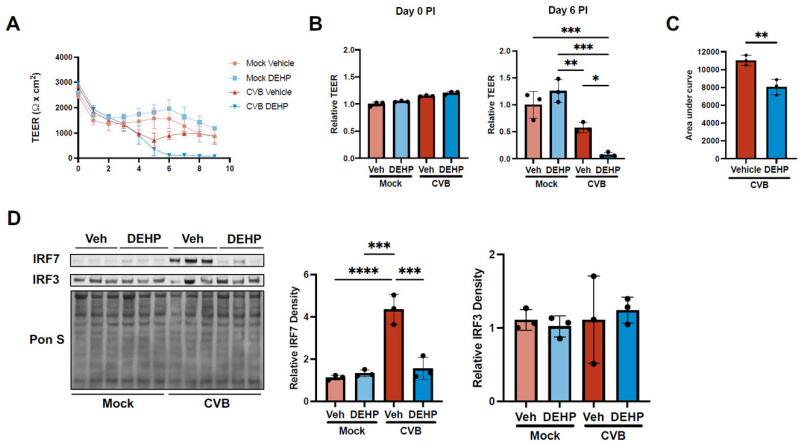

Figure 3. DEHP suppresses CVB-mediated interferon regulatory factor 7 induction in iBECs. **(A)** Transendothelial electrical resistance (TEER) measurements from iBECs treated with vehicle or DEHP prior to infecting with EGFP-CVB or mock-infecting. Daily raw TEER values from day 0 to day 9 post-infection (PI). **(B)** (Left) Relative TEER was recorded immediately after infecting cells (Day 0 PI). Values normalized to Day 0 PI Mock Vehicle group. (Right) Relative TEER recorded Day 6 PI. Values normalized to Day 6 PI Mock Vehicle group. **(C)** Area under the curve comparing overall TEER for Vehicle CVB and DEHP CVB groups **(D)** Western blots detecting IRF7 and IRF3 in iBECs treated with vehicle or DEHP prior to infecting with EGFP-CVB or mock-infecting for 48 hours. Pon S stain is shown below. Densitometric quantification of IRF7 and IRF3 are shown to the right (Student's t-test **(C)**, ANOVA **(B and D)**; n=3 per group; * p<0.05, ** p<0.01, *** p<0.001. Error bars represent standard deviation).

 doi:10.20944/preprints202409.1523.v1

DEHP Exacerbates CVB Infection by Enhancing Interferon-Induced Transmembrane 2 and 3 in HeLas and iBECs

Given that DEHP exposure may perturb virally-mediated interferon responses, we next interrogated if interferon-stimulated genes (ISGs) like interferon-induced transmembrane proteins (IFITMs) were affected by DEHP. IFITMs are a family of ISGs, and their expression is induced by type I interferons [31]. Both IFITM2 and 3 are generally thought to broadly inhibit viral infection, however their relationship with CVB is poorly-understood [32]. We performed western blots to assess IFITM2/3 protein levels in HeLas and iBECs following DEHP exposure and were surprised to find that they were increased with DEHP whether or not CVB was present (Figure 4A,B). To better understand how these IFITMs might impact CVB infection, we transfected HeLa cells with siRNA targeting either *IFITM2* or *IFITM3* prior to infecting with CVB. Silencing either of these genes substantially reduced infection as was indicated by decreased viral EGFP and intracellular VP1 levels (Figure 4C–E). Extracellular viral titers were also significantly lower with *siIFITM2* or *siIFITM3* compared to the control group (Figure 4F). These findings suggest that IFITM2 and 3 may actually support CVB infection, and that increased levels of these proteins may contribute to DEHP's proviral effects.

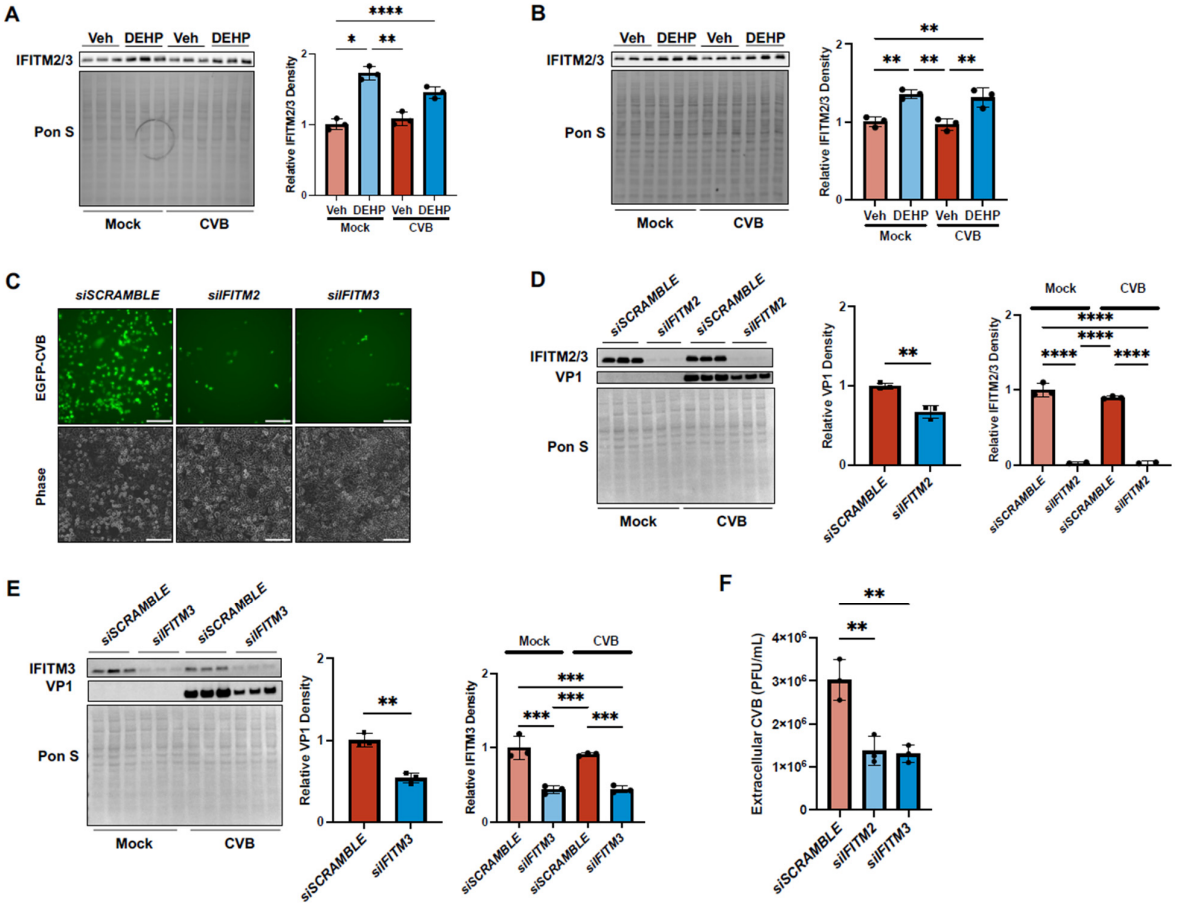

Figure 4. DEHP exacerbates CVB infection by enhancing interferon-induced transmembrane 2 and 3 in HeLas and iBECs. **(A and B)** Western blots detecting IFITM2/3 in HeLa **(A)** and iBECs **(B)** treated with vehicle or DEHP prior to infecting with EGFP-CVB or mock-infecting. Pon S stain is shown below. Densitometric quantification of IFITM2/3 is shown to the right. **(C)** Fluorescence microscopy detecting enhanced green fluorescent protein (EGFP) expression between cells transfected with scramble siRNA (*siSCRAMBLE)* (top), *IFITM2* siRNA (*siIFITM2*) (middle), or *IFITM3 siRNA* (*siIFITM3*) (bottom) for 48 hours prior to infecting with EGFP-CVB at MOI of 0.001 respectively for 24 hours (scale bars=100 μm). **(D)** Western blots detecting VP1 and IFITM2/3 in HeLas treated with

 doi:10.20944/preprints202409.1523.v1

siIFITM2 for 48 hours before infecting with EGFP-CVB at MOI of 0.001 respectively for 24 hours. Pon S stain is shown below. Densitometric quantification of VP1 and IFITM2/3 is shown to the right. **(E)** Western blots detecting VP1 and IFITM3 in HeLas treated with *siIFITM3* for 48 hours before infecting with EGFP-CVB at MOI of 0.001 respectively for 24 hours. Pon S stain is shown below. Densitometric quantification of VP1 and IFITM2/3 is shown to the right. **(F)** Viral plaque assays enumerating infectious viral titers in tissue culture media from cells in **C.** (Student's t-test **(D and E)**, ANOVA **(A, B, D, E, and F)**; n=3 per group; * p<0.05, ** p<0.01, *** p<0.001. Error bars represent standard deviation).

DEHP Has No Effect on Murine Cytomegalovirus Replication but Increases Group B Streptococcal Attachment and Invasion

Knowing that this pathway could potentially affect other viruses and some bacteria we tested the virus, cytomegalovirus (MCMV), and the bacteria, Group B Streptococcal (GBS). MCMV is a double-stranded DNA virus that establishes latency in mice and is used as a model of human CMV infection and spread [33–36]. Treating cells with 40 μg/mL DEHP did not impact MCMV replication in infected 10.1 mouse embryonic fibroblasts (Figure 5A), and there was no observable change in cytopathic effect. Additionally, we tested the effects of DEHP on GBS infection of iBECs. GBS is a common Gram-positive bacteria that colonizes the genitourinary and gastrointestinal tracts of 10-30% of pregnant women [37]. Peripartum infections are a major risk factors for potentially fatal neonatal meningitis unless antibiotics are appropriately administered [38]. We had previously demonstrated that iBECs are susceptible to GBS infection which results in significant disruption of barrier properties [27,28]. iBECs treated with 40 μg/mL DEHP prior to infecting with GBS significantly increased bacterial adherence and invasion (Figure 5B). These data suggest that DEHP can bolster some viral and bacterial infections, however the effects may be pathogen specific.

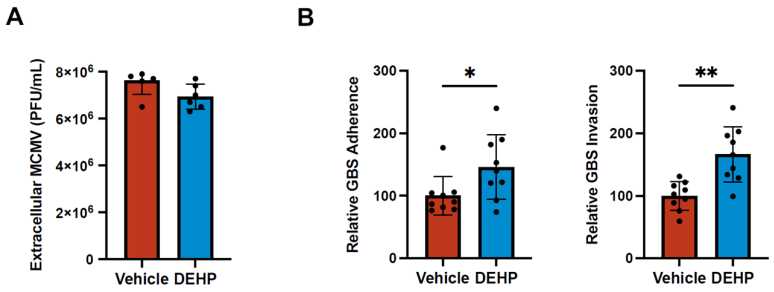

Figure 5. DEHP has no effect on murine cytomegalovirus replication but increases Group B Streptococcal attachment and invasion **(A)** Plaque assays enumerating infectious viral titers in tissue culture media from 10.1 mouse embryonic fibroblasts treated with vehicle or DEHP prior to infecting with MCMV at an MOI of 0.001. Supernatants were harvested and titered once 50% cytopathic effect was detected. **(B)** GBS adherence and invasion measurements on iBECs treated with vehicle or DEHP before infecting with GBS at an MOI of 10. Adherence and invasion were measured at 30 minutes and 2 hours PI respectively (Student's t-test; n=6 or 9 per group; * p<0.05, ** p<0.01, *** p<0.001. Error bars represent standard deviation).

Discussion

Recently, growing concerns have emerged regarding the accumulation of plasticizers and microplastics in the environment and the human health impacts they may have. DEHP is the most widely used member of the phthalate family of plasticizers with numerous studies identifying the chemical as an endocrine disruptor, probable carcinogen, and immunotoxicant [39–43]. Thus, DEHP exposure is associated with an increasing array of detrimental health manifestations; however very little is known about the impact DEHP has on infectious disease. In 2021, Lin et al. showed increased DEHP exposure exacerbated dengue virus infection and disease, and raises the question of whether DEHP could pose a risk for other pathogens [12].

 doi:10.20944/preprints202409.1523.v1

CVB infections commonly occur worldwide, and generally will result in subclinical illness. However, severe and sometimes fatal diseases such as aseptic meningoencephalitis, myocarditis, and pancreatitis can occasionally occur and are especially profound in very young children under the age of two years [14–16]. The risk factors associated with exacerbated CVB infections are poorly understood and generally thought to involve genetic, lifestyle, or environmental factors [17,18]. Elucidating these aspects could provide information as to why certain individuals exhibit higher susceptibility to severe CVB-induced illness.

In this study, we observe that DEHP can profoundly enhance CVB infection in a wide range of cultured cell types including HeLa cells, iBECs, Caco-2 cells, and HL-1s. In several of these cell types, we observe heightened viral spread as indicated by increased infected cell number and disproportionately higher amounts of extracellular virus compared to intracellular viral protein. Furthermore, our data suggest that DEHP may subvert virally-induced interferon signaling, and we hypothesize that this may contribute to exacerbated infection. Interestingly, we found that DEHP increases levels of IFITM2 and 3 and that these appear to be potentially proviral ISGs in the context of CVB infection. These particular IFITMs have been shown to have roles in endosomal and autophagosomal function during viral and bacterial infection [44–46]. We and others had previously reported that CVB can enter and hijack autophagosomes to facilitate vesicle-based viral egress, thus it is possible that these IFITMs may play a role in promoting these viral processes [47–50]. Nonetheless, further studies are needed to elucidate the role of these IFITMs during CVB infection, as very little is known about the relationship between CVB and IFITMs. Also surprising in this study was the observation that DEHP's effects appear to extend beyond just being proviral, as we also observed significantly increased adherence and invasion with GBS when DEHP is present.

There are likely numerous aspects that contribute to DEHP's proviral properties. For example, DEHP has been shown to increase the generation and accumulation of reactive oxygen species (ROS), and it has also been reported that ROS bolsters enteroviral replication [51,52]. On a similar note, it was reported that DEHP can disrupt mitochondrial dynamics and function, which not only could contribute to oxidative stress, but also impair mitochondria-resident antiviral machinery such as the nucleotide-binding domain, leucine-rich repeat-containing protein 3 (NLRP3) inflammasome and mitochondrial antiviral signaling (MAVS) protein [53,54]. Furthermore, as an extension of DEHP-mediated mitochondrial disruption, mitophagy has been demonstrated to be amplified as well, and we had previously reported that mitophagy is a crucial component of CVB egress via extracellular vesicles [55,56].

It is not clear how DEHP promotes CVB infection and GBS attachment and invasion. It will be important to elucidate mechanisms contributing to enhanced viral egress and suppressed cellular antiviral responses. Our data indicated that DEHP had no effect on MCMV infection which suggests that DEHP is not broadly proviral. Given that DEHP also promotes dengue virus infection (another RNA virus), it would be interesting to determine what effects DEHP has on RNA virus-specific immunity such as double-strand RNA surveillance. Additionally, it is unknown if a common pathway underlies the observed increases in both CVB and GBS infection following DEHP treatment, or if unrelated antiviral and antibacterial systems are impacted separately. In all, little is currently known about the impact DEHP has on infectious disease. Further interrogating the associated cellular mechanisms would be valuable in identifying whether this substance is a possible environmental risk factor for not only CVB infection but potentially for a larger range of viral and bacterial pathogens. Additionally, elucidating these DEHP-mediated mechanisms will no doubt help inform novel strategies to treat CVB-mediated diseases.

Supplementary Materials: The following supporting information can be downloaded at the website of this paper posted on Preprints.org.

Author Contributions: Conceptualization, R.K. and J.S.; Methodology, R.K., S.C., T.E.S., B.J.K., and J.S.; Validation, R.K., M.A., W.D.C., T.J.A, N.G.A., and J.S.; Investigation, R.K., M.A., W.D.C., T.E.K., S.C., T.J.A., N.G.A., T.E.S., B.J.K., and J.S.; Resources, T.E.S., B.J.K., and J.S.; Writing—Original Draft, R.K., W.D.C., T.E.K., N.G.A., T.E.S., B.J.K., and J.S.; Visualization, R.K., W.D.C., B.J.K., and J.S.; Supervision, R.K., T.E.S., B.J.K., and J.S.; Project Administration, R.K., T.E.S., B.J.K., and J.S.; Funding Acquisition, T.E.S., B.J.K., and J.S.

 doi:10.20944/preprints202409.1523.v1

Funding: JS is supported by National Institutes of Health (NIH) grant numbers R01DK125692 and R21AI145356. BJK is supported by NIH grant numbers R15NS131921 and R03AI185593. TS is supported by UT CMV Research Fund.

Acknowledgements: The authors would like to acknowledge Dr. Ralph Feuer (San Diego State University, CA, USA) for generously providing HeLa RW stocks and the pMKS1 plasmid, Dr. Roberta A Gottlieb (Cedars-Sinai Medical Center, CA, USA) for generously providing HL-1 stocks, Dr. Nicholas Lennemann (University of Alabama at Birmingham, AL, USA) for generously providing Caco-2 cells, and Morgan Hetzel for help with MCMV plaque assays.

Conflicts of Interest: The authors declare no competing interests.

References

1. Swift, L.M., et al., Evidence for the cardiodepressive effects of the plasticizer di-2-ethylhexyl phthalate. Toxicological Sciences, 2024. **197**(1): p. 79-94.
2. Jaeger, R.J. and R.J. Rubin, Extraction, localization, and metabolism of di-2-ethylhexyl phthalate from PVC plastic medical devices. Environ Health Perspect, 1973. **3**: p. 95-102.
3. Koch, H.M., R. Preuss, and J. Angerer, Di(2-ethylhexyl)phthalate (DEHP): human metabolism and internal exposure-- an update and latest results. Int J Androl, 2006. **29**(1): p. 155-65; discussion 181-5.
4. Melzak, K.A., et al., The Blood Bag Plasticizer Di-2-Ethylhexylphthalate Causes Red Blood Cells to Form Stomatocytes, Possibly by Inducing Lipid Flip-Flop. Transfusion Medicine and Hemotherapy, 2018. **45**(6): p. 413-422.
5. Greiner, T.O., et al., DEHP and its active metabolites: leaching from different tubing types, impact on proinflammatory cytokines and adhesion molecule expression. Is there a subsumable context? Perfusion, 2012. **27**(1): p. 21-9.
6. Chao, K.P., C.S. Huang, and C.Y. Wei, *Health risk assessments of DEHP released from chemical protective gloves.* Journal of Hazardous Materials, 2015. **283**: p. 53-59.
7. Demirel, A., et al., *Hidden Toxicity in Neonatal Intensive Care Units: Phthalate Exposure in Very Low Birth Weight Infants.* Journal of Clinical Research in Pediatric Endocrinology, 2016. **8**(3): p. 298-304.
8. Rose, R.J., et al., The effect of temperature on di(2-ethylhexyl) phthalate leaching from PVC infusion sets exposed to lipid emulsions. Anaesthesia, 2012. **67**(5): p. 514-520.
9. Aubuchon, J.P., T.N. Estep, and R.J. Davey, THE EFFECT OF THE PLASTICIZER DI-2-ETHYLHEXYL PHTHALATE ON THE SURVIVAL OF STORED RBCS. Blood, 1988. **71**(2): p. 448-452.
10. Zeng, G.W., et al., Low-level plasticizer exposure and all-cause and cardiovascular disease mortality in the general population. Environmental Health, 2022. **21**(1).
11. Liu, X.X., et al., Di-2-ethylhexyl phthalate (DEHP) exposure induces sperm quality and functional defects in mice. Chemosphere, 2023. **312**.
12. Lin, C.Y., et al., Mono-(2-ethylhexyl) phthalate Promotes Dengue Virus Infection by Decreasing IL-23-Mediated Antiviral Responses. Frontiers in Immunology, 2021. **12**.
13. Garmaroudi, F.S., et al., *Coxsackievirus B3 replication and pathogenesis.* Future Microbiology, 2015. **10**(4): p. 629-652.
14. Tracy, S., et al., Group B coxsackievirus myocarditis and pancreatitis:: Connection between viral virulence phenotypes in mice. Journal of Medical Virology, 2000. **62**(1): p. 70-81.
15. Sin, J., et al., Recent progress in understanding coxsackievirus replication, dissemination, and pathogenesis. Virology, 2015. **484**: p. 288-304.
16. Hu, Y.L., et al., Serostatus of echovirus 11, coxsackievirus B3 and enterovirus D68 in cord blood: The implication of severe newborn enterovirus infection. Journal of Microbiology Immunology and Infection, 2023. **56**(4): p. 766-771.
17. McManus, B.M., et al., Genetic determinants of coxsackievirus B3 pathogenesis, in Microarrays, Immune Responses and Vaccines, L. Aujame, et al., Editors. 2002. p. 169-179.
18. Drescher, K.M. and S.M. Tracy, *The CVB and etiology of type 1 diabetes*, in *Group B Coxsackieviruses*, S. Tracy, M.S. Oberste, and K.M. Drescher, Editors. 2008. p. 259-274.
19. Ianzini, F., et al., Lack of p53 function promotes radiation-induced mitotic catastrophe in mouse embryonic fibroblast cells. Cancer Cell Int, 2006. **6**: p. 11.
20. Lippmann, E.S., et al., Derivation of blood-brain barrier endothelial cells from human pluripotent stem cells. Nature Biotechnology, 2012. **30**(8): p. 783-791.
21. Espinal, E.R., S.J. Sharp, and B.J. Kim, Induced Pluripotent Stem Cell (iPSC)-Derived Endothelial Cells to Study Bacterial–Brain Endothelial Cell Interactions, in The Blood-Brain Barrier: Methods and Protocols, N. Stone, Editor. 2022, Springer US: New York, NY. p. 73-101.
22. Lippmann, E.S., et al., A retinoic acid-enhanced, multicellular human blood-brain barrier model derived from stem cell sources. Scientific Reports, 2014. **4**.

 doi:10.20944/preprints202409.1523.v1

23. Slifka, M.K., et al., Using recombinant coxsackievirus B3 to evaluate the induction and protective efficacy of CD8+ T cells during picornavirus infection. J Virol, 2001. **75**(5): p. 2377-87.
24. Gillum, N., et al., Clinically relevant concentrations of di (2-ethylhexyl) phthalate (DEHP) uncouple cardiac syncytium. Toxicol Appl Pharmacol, 2009. **236**(1): p. 25-38.
25. Posnack, N.G., et al., Gene expression profiling of DEHP-treated cardiomyocytes reveals potential causes of phthalate arrhythmogenicity. Toxicology, 2011. **279**(1-3): p. 54-64.
26. Jackson, J.W., et al., Anticytomegalovirus Peptides Point to New Insights for CMV Entry Mechanisms and the Limitations of In Vitro Screenings. mSphere, 2019. **4**(1).
27. Kim, B.J., et al., Modeling Group B Streptococcus and Blood-Brain Barrier Interaction by Using Induced Pluripotent Stem Cell-Derived Brain Endothelial Cells. mSphere, 2017. **2**(6).
28. Vollmuth, N., et al., Group B Streptococcus transcriptome when interacting with brain endothelial cells. Journal of Bacteriology, 2024. **206**(6).
29. Espinal, E.R., et al., Group B Streptococcus-Induced Macropinocytosis Contributes to Bacterial Invasion of Brain Endothelial Cells. Pathogens, 2022. **11**(4).
30. Mamana, J., et al., Coxsackievirus B3 infects and disrupts human induced-pluripotent stem cell derived brain-like endothelial cells. Frontiers in Cellular and Infection Microbiology, 2023. **13**.
31. Müller, U., et al., Functional role of type I and type II interferons in antiviral defense. Science, 1994. **264**(5167): p. 1918-21.
32. Takaoka, A. and H. Yanai, *Interferon signalling network in innate defence.* Cellular Microbiology, 2006. **8**(6): p. 907-922.
33. Fisher, M.A. and M.L. Lloyd, A Review of Murine Cytomegalovirus as a Model for Human Cytomegalovirus Disease-Do Mice Lie? Int J Mol Sci, 2020. **22**(1).
34. Roback, J.D., et al., Transfusion-transmitted cytomegalovirus (CMV) infections in a murine model: characterization of CMV-infected donor mice. Transfusion, 2006. **46**(6): p. 889-95.
35. Jordan, M.C., INTERSTITIAL PNEUMONIA AND SUB-CLINICAL INFECTION AFTER INTRANASAL INOCULATION OF MURINE CYTOMEGALOVIRUS. Infection and Immunity, 1978. **21**(1): p. 275-280.
36. Brizić, I., et al., *Cytomegalovirus Infection: Mouse Model.* Curr Protoc Immunol, 2018. **122**(1): p. e51.
37. Brigtsen, A.K., et al., Group B Streptococcus colonization at delivery is associated with maternal peripartum infection. PLoS One, 2022. **17**(4): p. e0264309.
38. Tavares, T., L. Pinho, and E. Bonifácio Andrade, *Group B Streptococcal Neonatal Meningitis.* Clin Microbiol Rev, 2022. **35**(2): p. e0007921.
39. Ernst, J., et al., The endocrine disruptor DEHP and the ECS: analysis of a possible crosstalk. Endocrine Connections, 2020. **9**(2): p. 101-110.
40. Heudorf, U., V. Mersch-Sundermann, and J. Angerer, *Phthalates: toxicology and exposure.* Int J Hyg Environ Health, 2007. **210**(5): p. 623-34.
41. Yang, L., et al., Exposure to di-2-ethylhexyl phthalate (DEHP) increases the risk of cancer. BMC Public Health, 2024. **24**(1): p. 430.
42. Zhang, Y., et al., *Health risks of phthalates: A review of immunotoxicity.* Environ Pollut, 2022. **313**: p. 120173.
43. Wang, S., et al., DEHP induces immunosuppression through disturbing inflammatory factors and CYPs system homeostasis in common carp neutrophils. Fish Shellfish Immunol, 2020. **96**: p. 26-31.
44. Narayana, S.K., et al., The Interferon-induced Transmembrane Proteins, IFITM1, IFITM2, and IFITM3 Inhibit Hepatitis C Virus Entry. Journal of Biological Chemistry, 2015. **290**(43): p. 25946-25959.
45. Ranjbar, S., et al., A Role for IFITM Proteins in Restriction of Mycobacterium tuberculosis Infection. Cell Reports, 2015. **13**(5): p. 874-883.
46. Shi, G., O. Schwartz, and A.A. Compton, More than meets the I: the diverse antiviral and cellular functions of interferon-induced transmembrane proteins. Retrovirology, 2017. **14**(1): p. 53.
47. Kemball, C.C., et al., Coxsackievirus infection induces autophagy-like vesicles and megaphagosomes in pancreatic acinar cells in vivo. J Virol, 2010. **84**(23): p. 12110-24.
48. Robinson, S.M., et al., Coxsackievirus B Exits the Host Cell in Shed Microvesicles Displaying Autophagosomal Markers. Plos Pathogens, 2014. **10**(4).
49. Sin, J., et al., Coxsackievirus B Escapes the Infected Cell in Ejected Mitophagosomes. Journal of Virology, 2017. **91**(24).
50. Chen, Y.H., et al., Phosphatidylserine Vesicles Enable Efficient En Bloc Transmission of Enteroviruses. Cell, 2015. **160**(4): p. 619-630.
51. Cheng, M.L., et al., Enterovirus 71 induces mitochondrial reactive oxygen species generation that is required for efficient replication. PLoS One, 2014. **9**(11): p. e113234.
52. Cheng, M.L., et al., Enteroviral 2B Interacts with VDAC3 to Regulate Reactive Oxygen Species Generation That Is Essential to Viral Replication. Viruses, 2022. **14**(8).
53. Chen, S., et al., TBK1-Mediated DRP1 Targeting Confers Nucleic Acid Sensing to Reprogram Mitochondrial Dynamics and Physiology. Mol Cell, 2020. **80**(5): p. 810-827.e7.

 doi:10.20944/preprints202409.1523.v1

54. Park, S., et al., Defective mitochondrial fission augments NLRP3 inflammasome activation. Sci Rep, 2015. **5**: p. 15489.
55. Chatterjee, S., R. Kordbacheh, and J. Sin, Extracellular Vesicles: A Novel Mode of Viral Propagation Exploited by Enveloped and Non-Enveloped Viruses. Microorganisms, 2024. **12**(2).
56. Sawaged, S., et al., TBK1 and GABARAP family members suppress Coxsackievirus B infection by limiting viral production and promoting autophagic degradation of viral extracellular vesicles. Plos Pathogens, 2022. **18**(8).